# Thermal and visual comfort analysis of adaptive vacuum integrated switchable suspended particle device window for temperate climate


Srijita Nundy[1] Aritra Ghosh[2]*

[1]School of advanced materials science and engineering, Sungkyunkwan University, Suwon 16419, Republic of Korea

[2]Environmental and Sustainability Institute, University of Exeter, Penryn, Cornwall, TR10 9FE, UK

*Corresponding author: a.ghosh@exeter.ac.uk ; aritraghosh_9@yahoo.co.in


## Nomenclature

| | |
|---|---|
| $A_g$ | Area of glazing ($m^2$) |
| $C_{air}$ | Specific heat of air (kJ/kg K) |
| $F_{sd}$ | Skin damage factor |
| I | Incident radiation ($W/m^2$) |
| $I_{cl}$ | Thermal resistance of clothing ($m^{2\,0}C/W$) |
| $k_g$ | Thermal conductivity of glass ($W/m^2K$) |
| $L_g$ | Thickness of glass (m) |
| $L_{polystyrene}$ | Thickness of polystyrene (m) |
| M | Metabolic rate in ($W/m^2$) of the body surface area |
| $M_{test\ cell}$ | Mass of the air inside test cell (kg) |
| $T_{ambient}$ | Ambient room temperature (K) |
| $T_{pv}$ | Temperature of PV cell (K) |
| $T_{testcell}$ | Test cell temperature (K) |
| p | Pillar spacing |
| $P_a$ | Water vapour partial pressure (Pascal) |
| $V_{air}$ | Relative air velocity |
| W | Effective mechanical power, equal to zero for most effectives |
| $\tau$ | transmissivity |
| $\beta$ | Packing factor |
| $\beta_0$ | Temperature coefficient of PV |
| $h_c$ | Convective heat transfer coefficient ($W/m^2K$) |
| $t_a$ | Air temperature ($^0C$) |
| $f_{cl}$ | Ratio of surface area of the body with clothes to the surface area of the body without clothes |
| $t_{cl}$ | Clothing surface temperature |
| $t_{rm}$ | Mean radiant temperature |
| $\tau_{da}$ | CIE damage factor |

## Highlights:

- Spectral measurement of combined suspended particle device-vacuum glazing provided 38% transmission while 110V AC was supplied.
- Thermal comfort of suspended particle device-vacuum combined glazing was evaluated using PMV and PPD methods
- Visual comfort was calculated using useful daylight, daylight glare and colour properties

**Abstract:**

In this work, thermal and visual comfort of low heat loss switchable suspended particle device-vacuum (SPD-vacuum) glazing was investigated for less energy-hungry adaptive building's glazing or façade integration at temperate climate. This SPD-vacuum glazing had 38% visible transmittance in the presence of 110 V applied an alternating voltage and 2% visible transmittance in the absence of electrical power. Outdoor test cell characterisation was employed to measure the thermal and daylighting parameters of this glazing. Solar heat gain or solar factor was calculated using non calorimetric methods and varied between 0.38 (Switch OFF/opaque) to 0.51 (Switch ON/ transparent). Test cell indoor and ambient parameters (incident solar radiation and ambient temperature) were engaged for thermal comfort analysis by using PMV and PPD methods. Visual comfort was analysed from glare potential, useful daylight index, and colour properties. The comfortable thermal environment was attainable using both states of this glazing for a clear sunny day. Acceptable daylight throughout the day was possible for a clear sunny day for opaque state; however clear state offered allowable/comfortable correlated colour temperature (CCT) of 5786.18 K and colour rendering index (CRI) of 94.83.

Keywords: SPD, vacuum, thermal comfort, test cell, temperature, transmission, glazing

## 1. Introduction

Buildings are intricate and durable consumer goods, which protect from the adverse external environment by offering shelter and brings natural light, fresh air to ensure the sustainability of the living environment. High-performance buildings are getting priority as consumption of world energy specifically in the building sector has been increased alarmingly due to economic development, urbanization, an increase of living standard, length of stay in the building. The diurnal or seasonal outdoor environment and the continuing conundrum of the built environment promote the higher building energy consumption. Building occupants prefer a comfortable indoor environment that directly impacts their productivity and cognitive performance, health and well-being [1]. Therefore, thermal [2] and optical/visual comfort [3] are the two primary criteria to understand the comfort level of buildings' occupants [4]. In a building, windows are the most crucial envelope by limiting or allowing solar energy and daylight and viewing from indoor to outdoor. To maintain visual comfort, most often large-scale transparent envelope is installed which in turn enables excessive heat gain or excessive heat loss. These highly transparent windows are the weakest part of an energy-efficient or less energy-hungry building [5]. Improved energy performance can be pursued through the integration of energy-efficient smart switchable window [6–9].

Switchable glazing materials provide a minimum of two transmittance states which makes them competent to combat with diurnal nature of ambient over static single transparent glazing [10]. Switchable glazing material can be switched from one state to another by, thermal, optical, mechanical, or electrical stimuli. Thermochromic [11], thermotropic and phase change material [12] are the thermally actuated switchable glazing material while optically activated photochromatic [13] changes its state in the presence of light. Mechanically actuated switchable materials include micro-wrinkles from elastomeric polymers, particle embedded elastomer composite, silica particles embedded in a poly(dimethylsiloxane) (PDMS) film [14] types. Electrically actuated electrochromic (EC) [12], suspended particle devices (SPD) [15,16], and polymer dispersed liquid crystal (PDLC)[17,18] [19] are advantageous for their controllable optical transmission to meet occupants demand. SPD type electrically activated glazing as shown in Figure 1 is promising over EC for its fast switching and promising over PDLC for its no diffuse transmission property [20].

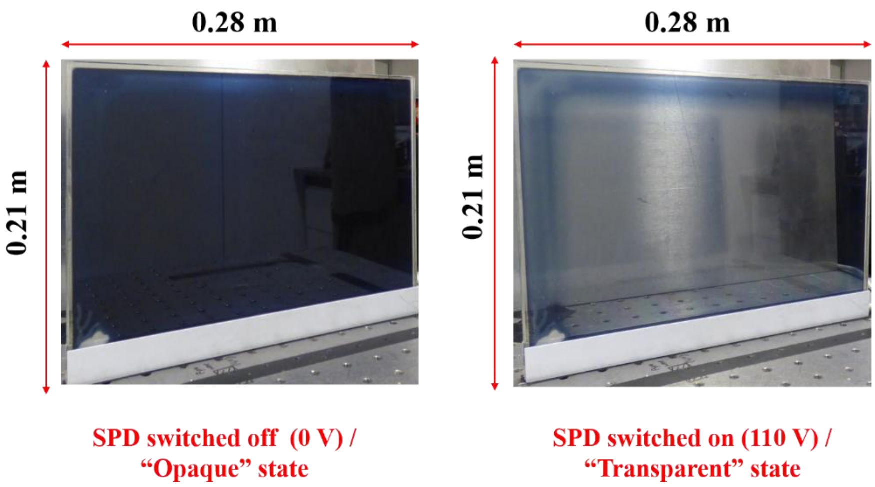


Figure 1: Photograph of an electrically activated switchable suspended particle device (SPD) glazing showing opaque and transparent state.

Suspended particle device (SPD) contains rod-shaped, needle-shaped, or lath-shaped heraphathite or dihydrocinchonidine bisulfite polyiodide types particles [21]. In the presence of the applied electric field, SPD becomes transparent or ON state because particles become aligned and most of the light can pass through the device [22]. However, in the absence of an applied electrical field, SPD is relatively dark, and this state is known as OFF state. The reason behind this phenomenon is due to particles random Brownian movement in the liquid suspension when no power is applied. In this state, a beam of light passing into the device is rejected, transmitted or absorbed depending upon the device structure, the nature of particles, concentration of the particles and the energy content of the light which makes this dark [23]. Plastic films are suitable for window application over liquid suspension because it does not noticeably agglomerate when the film is repeatedly activated with a voltage and eliminates the bulging effect from hydrostatic pressure of a high column suspension and leakage possibility from the device. Research Frontiers Inc (RFI) is the only commercial developer of SPD devices that produces goggles, eyeglasses and windows. Light transmission of SPD can vary from 0.1 to 60%, with a switching speed of 100 to 200 ms [24]. Thermal [25,26], daylighting [16,27,28] and electrical [24,29] analysis of SPD glazing using outdoor test cells at temperate climate showed that this is suitable for retrofit or new net zero energy building. Indoor optical characterisation confirmed low or negligible diffused transmission of SPD glazing [22] compared to any PDLC [30,31] material.

To control building heating load, multiple-pane glazing [32], aerogel [33,34] filled or vacuum glazing [35] are the investigated advanced glazing systems. However, multiple-pane glazing offers heavyweight, which makes it less suitable for retrofit construction. On the other hand, aerogel glazing blocks the direct views from the interior to the exterior and direct incident solar radiation creates accentuated reflection and glare. Thus, to obtain lower transmission without compromising visible transmittance, insulated vacuum glazing is an option [36][37,38] as shown in Figure 2. In a vacuum glazing, between two glass sheets, reduction of atmospheric-air mass creates a vacuum at high – pressure (0.13 Pa–$1.33 \cdot 10{-}4$ Pa) [39]. Presence of small support pillars, typically have radii from 0.1 mm to 0.2 mm and height of 0.1 mm–0.2 mm, between two glass, counteract the pressure difference of external atmospheric-air and internal vacuum pressure [40]. Low-density air reduces conductive and convective heat transfer, and use of low emissivity coating reduces the radiative heat transfer [41]. To maintain a vacuum, edges of glass sheets are sealed hermetically [42] by low-temperature indium alloy edge sealing techniques [43,44]. This low-temperature process enables soft low emission coating and tempered glass to be used compared to high-temperature solder glass edge sealing [45,46] technique which degrades the soft low emission coating and tempered glass. Indoor characterisation of vacuum glazing under a controlled environment using hotbox calorimeter [47], simulation work using finite elements [48], and outdoor thermal [36], optical [49] and daylighting [36] characterisation using outdoor test cell at temperate climate were investigated earlier, which confirmed that insulated vacuum glazing is suitable for low energy building application. Transmitted daylight through vacuum glazing also offers high colour render [28,50] for colour comfort of buildings occupants.

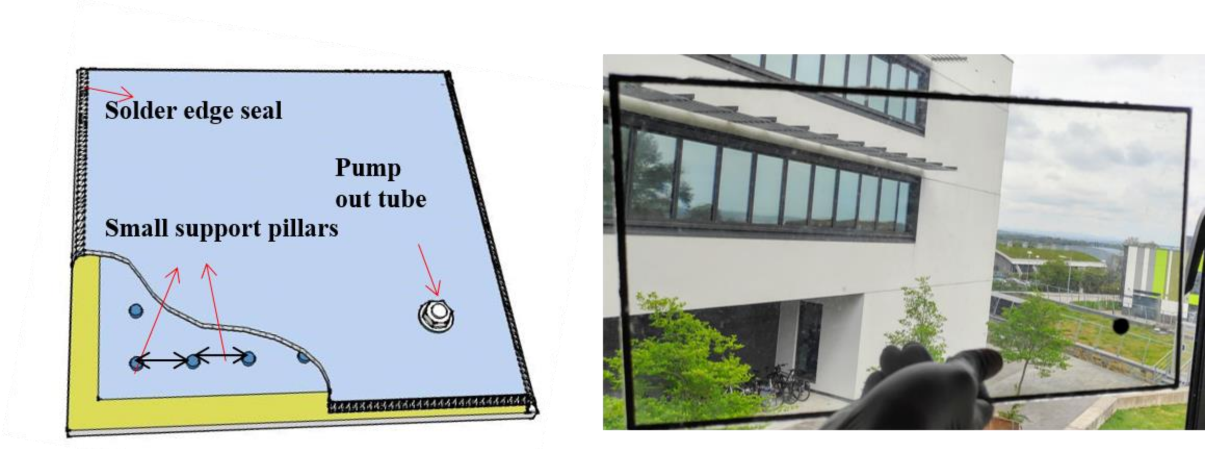


(a) (b)

Figure 2: (a) Schematic and (b) viewing through an Evacuated glazing.

For temperate and cold climate daylight glare is an issue that can be eliminated by using an additional coloured coating. However, the addition of this fixed transmittance is not suitable for controlling of diurnal behaviour of external ambient. Switchable glazing material which has at least two transmittances, can be the best option. Addition of switchable glazing with vacuum glazing provides low heat loss switchable glazing as shown in Figure 3 and reported by [51,52]. This combined system's transmission varied from 2% to 38% in the presence of 110 V alternating power supply while solar heat gain changed from 4% to 27% [51].

Providing thermal comfort and visual comfort by using advanced low heat loss switchable glazing can reduce the necessity of heating, ventilation and air-condition (HVAC) and artificial lighting loads. The Predicted Mean Vote (PMV) and Percentage People Dissatisfied (PPD) method have been used worldwide to predict and assess building's interior thermal comfort which became an international standard in 1980 [53]. However, investigated work using thermal comfort evaluation for glazing system is limited and only a few published works are available. Thermal comfort was evaluated using fifteen different 3 mm single glazed clear glass to double glazed with low emission (low-e) and solar control coating. For cold climate all glazing type except solar control and for hot climate solar control glazing was suitable to offer human thermal comfort [54]. Clear glass, tinted glass, reflective glass, double pane glass, and low-e glass were investigated for Bangkok climate where discomfort occurred when single pane glazing was employed [55]. PV double-glazing window integrated with amorphous-Si PV panel reduced indoor heat gain and cooling load significantly by setting up an air gap behind PV modules and provided the best thermal comfort over PV single-glazing window [56].

Optical or visual comfort of a glazing system is determined by incoming illuminance and colour properties of daylight. Bright ambient daylighting is required as it closely associated with cognitive activation [57,58]. Excessive daylight illuminance offers glare which can be evaluated by daylight glare control whilst colour properties evaluation includes correlated color temperatures (CCT) and color rendering index (CRI). Glare analysis and colour properties of switchable glazing have already been done using EC [59], SPD [27] and PDLC [60] type glazing. EC glazing showed excellent control over glare for its opaque and transparent state while SPD glazing showed 30% transmission was suitable for indoor visual comfort. PDLC glazing's high diffuse transmission in its both transparent and translucent states were incapable to control higher indoor illuminance for a clear sunny day whilst it's colour properties were suitable for interior. However, PDLC's switched OFF state blocks direct solar radiation.

The performance of combined SPD-vacuum technologies is not satisfactorily understood as that of SPD and vacuum glazing. In this work for the first-time visual comfort and thermal comfort of SPD-vacuum combined glazing were investigated and reported.

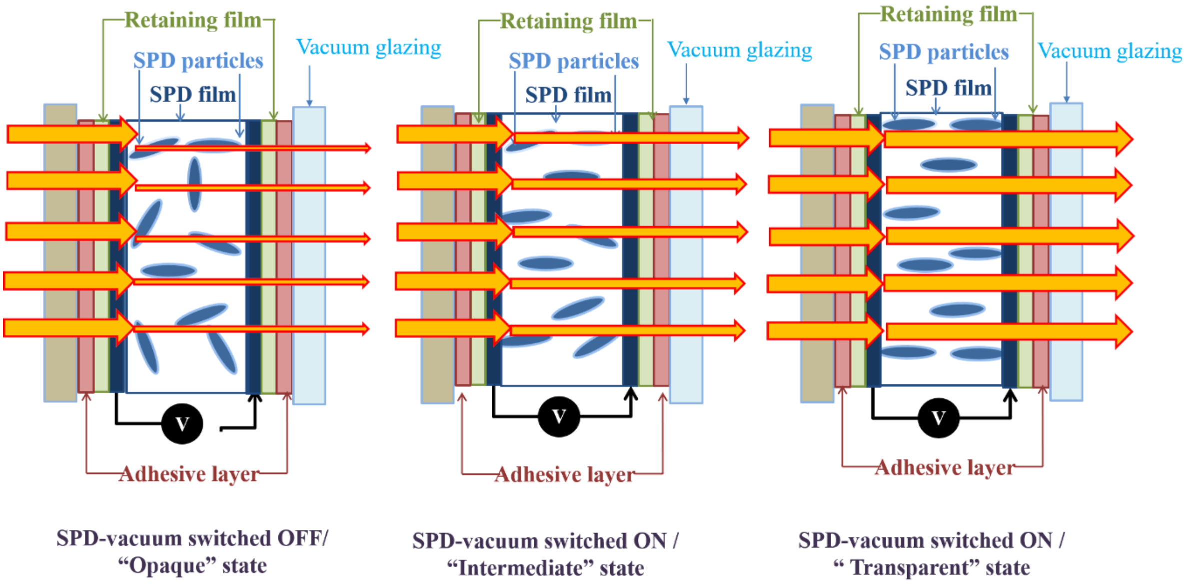


Figure 3: Schematic of combined SPD-vacuum glazing at different switching states.

## 2. Methodology

For thermal and visual comfort analysis, an experiment was performed from the 1$^{st}$ of April to the 1$^{st}$ of September 2016 in Dublin Ireland (53.34 $^0$N, 6.25 $^0$W). Following the Köppen-Geier classification, this location is temperate climate and more precisely temperate oceanic climate [61,62]. In a temperate climate, yearly mean temperatures are neither extremely cold nor hot and generally it is the area between the subtropics and the polar circles. Temperate climates zones have mean ambient temperatures above than−3 °C and lower than 18 °C [63]. Climatic data for this particular location is shown in Figure 4 which includes average monthly solar radiation, mean ambient, mean precipitation and mean wind speed. Annual horizontal plane total global solar radiation was 3677.85, 3502.12, 3490.24 MJ/m$^2$ for the year of 2014, 2015 and 2016 respectively as shown in Figure 4a. Dublin's climate is the proximity of the westerly atmospheric circulation and Atlantic Ocean (and the Gulf Stream) which ensures that this location is dominated by maritime influences. Precipitation occurred maximum of 180 mm and a minimum 20 mm between 2014 to 2016. Mean annual wind speed was consistently high, with mean values of 10 knot in the northwest direction. This location (Dublin, Ireland) has a similar climate to countries such as the United Kingdom (Wales and mid/North England), Belgium, northern Germany, Netherlands, Sweden, Denmark and the Baltic States (Estonia, etc.)[64].

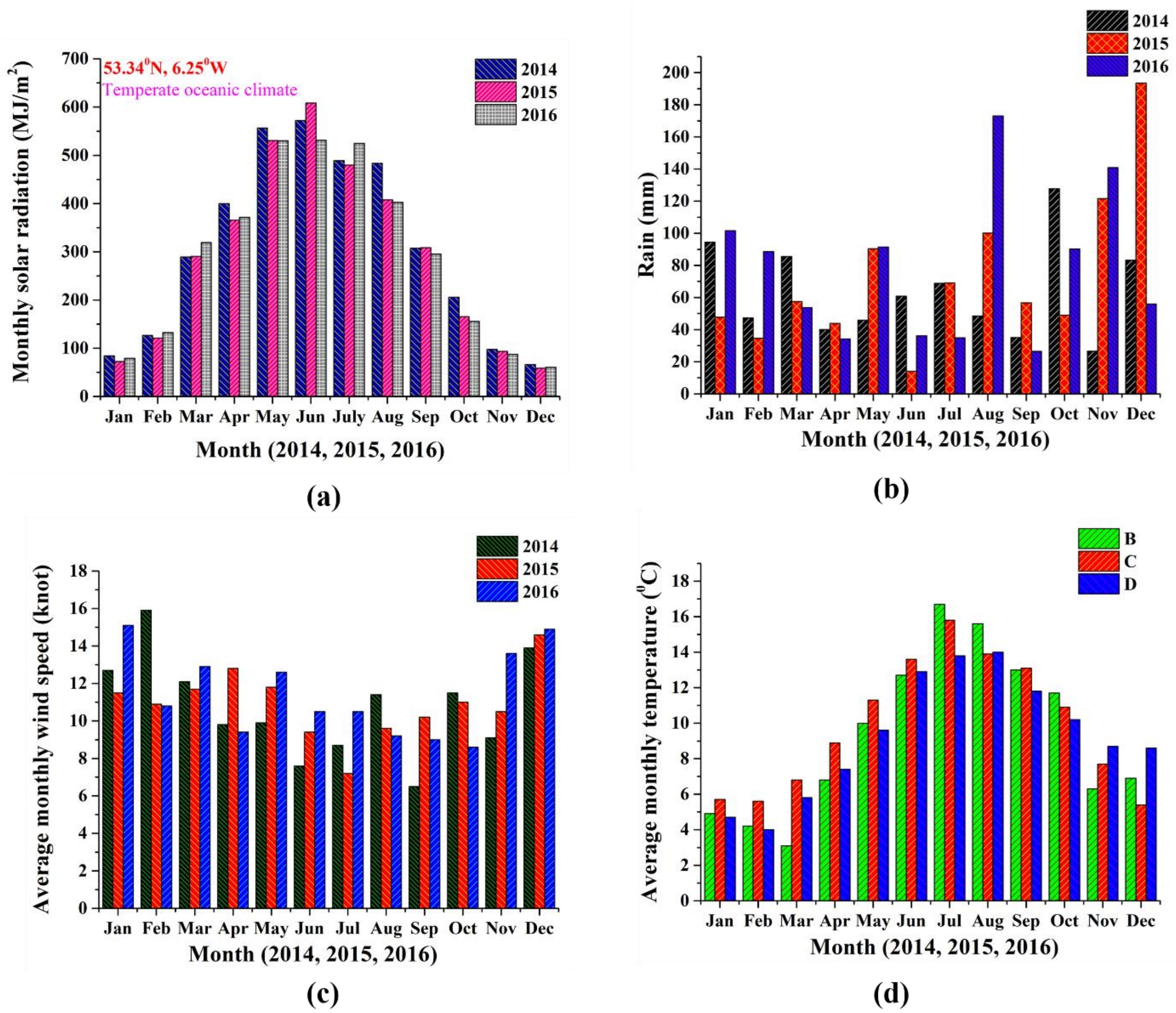


Figure 4: Monthly average solar radiation, rain, wind speed and average temperature for the year of 2014, 2015, 2016 at a temperate oceanic climate (53.34 $^{0}$N, 6.25 $^{0}$W).

A 0.7 (l) × 0.7 m (w) × 0.07 m (h) test cell was developed by using wood and 0.15 m thick polystyrene insulation material. The area of glazing and the test cell was in a ratio of 1:9 while internal surfaces were painted with 0.8 reflectance matt white paint for this research work. The test cell was placed under exposure of unobstructed solar illuminance. Window occupied 35% of the wall of the test cell which gave a window to wall ratio of 1:3.5. Details of the experiment set up can be found from previously reported work [27,36]. Data were recorded at 1 min intervals using delta T data type logger. For thermal comfort evaluation, only clear sunny day results were considered while for visual comfort characterisations were performed as functions of time, clear, intermittent cloudy and overcast type cloudy day. Both experiments were performed for south-facing test cells and ‘transparent’ and ‘opaque’ switching states. Details of investigated glazing systems are mentioned in Table 1.

Table 1: Details of glazing systems

| | | Dimensions (m × m) | Power supply | Supplier |
|---|---|---|---|---|
| Glazing | Vacuum | 0.35 × 0.2 | Not required | NSG |
| | SPD | 0.28 × 0.21 | 110 V (50 Hz AC sinusoidal signal); (Transparent) | Smart Glass International |
| | | | 0 V (Opaque) | |

## 2.1. Thermal comfort

Temperature swing inside a building occurs due to the diurnal nature of ambient. However, humans prefer to stay in a constant or nearly constant comfortable room temperature between 18 $^0$C-20 $^0$C [65], which offers thermal comfort. The temperature difference between exterior and interior leads to the asymmetrical thermal environment and a variety of thermal comfort level. Thermal comfort influencing factors are solar heat gain and heat loss, which are determined by solar heat gain coefficient (SHGC) and overall heat transfer coefficient (*U*-value). The SHGC represents transmitted solar radiation in addition to the absorbed and re-emitted solar radiation inside a building due to glazing and its values vary between 0 to 1. For colder climate and winter season, high SHGC is effective while blocking of SHGC is required for hotter climate and summer season.

Solar factor (g) or solar heat gain coefficient is given by equation 1 where $h_e$ and $h_i$ are the external and internal heat transfer coefficient, $\tau_s$ is solar transmittance and $\rho_s$ is solar reflectance [66].

$$g = \tau_s + q_i = \tau_s + \alpha \frac{h_i}{h_i + h_e} = \tau_s + (1 - \tau_s - \rho_s)\frac{h_i}{h_i + h_e} \quad (1)$$

Light to solar gain (LSG) indicates higher daylight in a room while SHGC is less [67]. Selectivity index (equation 2) is the ratio of light transmissivity with total energy transmittance of glazing. For solar control glazing, higher selective coefficients are potential.

$$LSG = \frac{VT}{SHGC} = Selectivity\ index \quad (2)$$

Solar material protection factor (SMRF) is given by

$$SMRF = 1 - \tau_{da} = 1 - \frac{\sum_{\lambda=300nm}^{600nm} T(\lambda) C_\lambda S_\lambda \Delta\lambda}{\sum_{\lambda=300nm}^{600nm} C_\lambda S_\lambda \Delta\lambda} \quad (3)$$

where $C_\lambda = e^{-0.012\lambda}$ , $\tau_{da}$ is CIE damage factor, and solar skin protection factor (SSPF) is given by

$$SSPF = 1 - F_{sd} = 1 - \frac{\sum_{\lambda=300nm}^{400nm} T(\lambda) E_\lambda S_\lambda \Delta\lambda}{\sum_{\lambda=300nm}^{400nm} E_\lambda S_\lambda \Delta\lambda} \quad (4)$$

$E_\lambda$ CIE erythermal effectiveness spectrum and $F_{sd}$ is skin damage factor

The index termed predicted mean vote (PMV) is applied to evaluate the indoor thermal comfort level, and it is expressed by equation 5. The advantage of the PMV model is that it is a flexible tool that includes all the major variables influencing thermal sensatione e.g. air temperature, mean radiant temperature, relative humidity, air movement, clothing insulation, and metabolic rate. The PMV model also suitable for cold climate. Table 2 indicates the different range for thermal comfort while Table 3 shows the list of assumed parameters were employed in this work to calculate thermal comfort [53,54].

$$PMV = \left(0.303e^{-0.036M} + 0.028\right) \times \begin{Bmatrix} (M-W) - 3.05\times10^{-3} \times \left[5733 - 6.99(M-W) - P_a\right] \\ -(0.42)\times\left[(M-W) - 58.15\right] - 1.7\times10^{-5} M\left(5867 - P_a\right) - 0.0014M\left(34 - t_a\right) \\ -(3.96)\times10^{-8} \times f_{cl} \times \left[\left(t_{cl}+273\right)^4 - \left(t_{rm}+273\right)^4\right] - f_{cl}h_c\left(t_{cl} - t_a\right) \end{Bmatrix} \quad (5)$$

$$PPD = 100 - 95\times\exp\left(-0.03353\times PMV^4 - 0.2179\times PMV^2\right) \quad (6)$$

Table 2: Thermal sensation vote or thermal comfort level for indoor temperature [68,69]

| Sensation | Scale value |
|---|---|
| Hot | +3 |
| Warm | +2 |
| Slightly warm | +1 |
| Neutral | 0 |
| Slightly cool | -1 |
| Cool | -2 |
| Cold | -3 |

Table 3: Assumption for thermal comfort evaluation [68,69]

| Detail of the input parameter | Details of dimension and values |
|---|---|
| Room Dimension | 5 m × 5 m × 5 m; The person is seated 1m away from the window which occupies entire external (5 m × 5 m).<br>Window here means only glazing without frame. |
| Clothing insulation ($I_{cl}$) | 0.5 Summer<br>1 winter |

| | |
|---|---|
| Metabolic rate (M) | 1.2 summer<br>1.0 winter<br>Relaxed seated person is 1 |
| External work (W) | 0 |
| Solar absorptance of a person | 0.6 |
| Emittance of human body | 0.97 |
| Projected area factor of person | 0.3 |
| Water vapour pressure (Pa) | 1587 Pascal (kg/m$^2$s$^2$) |

## 2.2. Visual comfort

Quality and quantity of indoor daylight determine the visual comfort for an interior. Quantity of daylight is represented or evaluated by daylight glare and incoming illuminance while the quality of daylight is defined by CRI and CCT. Amount of acceptable entering illuminance into an interior can be varied between 100 and 2000 lux which is widely known as useful daylight illuminance (UDI) [70]. UDI <100 lux, is unacceptable and provide discomfort, while 100 lux ≤ illuminance ≤ 2000 lux indicate most useful and allows comfort and UDI> 2000 lux indicate excessive daylight or glare. Excessive entering direct illuminance creates discomfort glare. Subjective rating (SR) [71] and daylight glare index ($DGI_N$) [72] are employed to find out discomfort level. Subjective rating (SR) glare control for SPD-vacuum glazing was identified as the best choice to evaluate glare potential as it only engages one photo sensor and using measured outdoor illuminance. This SR (is given by equation 7) index allows discomfort glare estimation experienced by subjects when working at a visual daylight task (VDT) placed against a window of high or non-uniform luminance [71].

$$SR = 0.1909 E_v^{0.31} \quad (7)$$

To find daylight glare index, due to large glare sources such as light coming through windows, $DGI_N$ is the best choice as given in equation 8 [73,74]. Table 4 shows the different criteria level for $DGI_N$ and criterion scale of discomfort glare subjective rating (SR) (Lee and DiBartolomeo, 2002)

$$DGI_N = 10 \log_{10} 0.478 \sum_{i=1}^{n} \frac{L_{ext}^{1.6} \Omega_{pN}^{0.8}}{L_{adp} + 0.07 \omega_N^{0.5} L_{win}} \quad (8)$$

Where $L_{win}$ is window luminance (cd/m$^2$) and $L_{adp}$ is adaptation luminance of the surroundings including reflections from an internal surface (cd/m$^2$). $L_{ext}$ is the exterior luminance of the outdoor source including direct sunlight, diffuse skylight and reflected light from the ground and other external surfaces (cd/m$^2$), $\omega_N$ solid angle subtended by the window, $\Omega_{pN}$ solid angle subtended by the glare source.

Table 4: Glare level for DGI and SR (Wienold, 2009)

| | | Daylight glare index (DGI) | Glare subjective rating (SR) |
|---|---|---|---|
| *Level of light* | Just perceptible | 16 | |
| | Perceptible | 18 | |
| | Just acceptable | 20 | 0.5 |
| | Acceptable | 22 | |
| | Just uncomfortable | 24 | 1.5 |

| | | | |
|---|---|---|---|
| | Uncomfortable | 26 | |
| | Just intolerable | 28 | 2.5 |

For SR calculation internal vertical illuminance ($E_V$) facing the window (worst case) was measured at the centre of the room. Table 4 listed the different glare level for DGI and SR. This method also allows the non-intrusive measuring equipment necessary for scale model daylighting assessments [75,76]. For $DGI_N$ four illuminance sensors were used, one on the vertical surface of the outside surface of the test cell and three inside the test cell. All illuminance sensors had a 350 nm-820 nm sensitivity spectral range adapted to human eye sensitivity. Horizontal measurements were made 27 cm distant from the glazing inner surface as shown in Figure 5. Horizontal illuminances on a work plane inside the test cell and daylight glare index ($DGI_N$) were investigated using SPD-vacuum glazing transparent/switch on and translucent/ switch off conditions in the temperate climate for three days with different prevailing weather conditions.

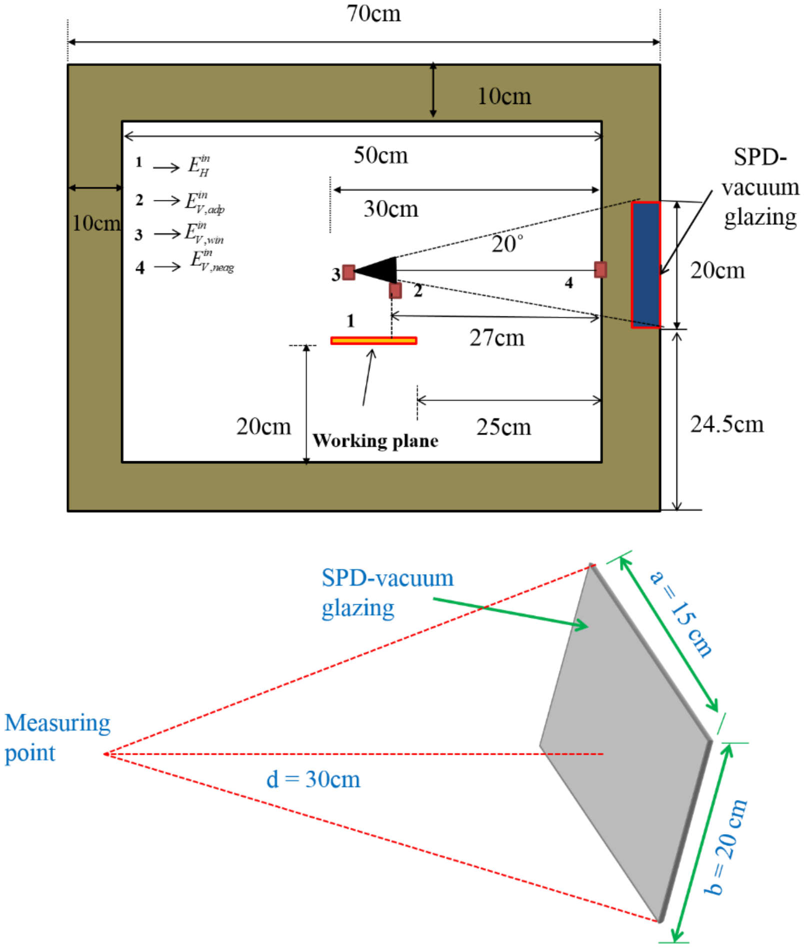


Figure 5: Schematic experimental cross section of an unfurnished room integrated switchable low heat loss SPD-vacuum glazing place on vertical south for the calculation of SR and $DGI_N$ with configuration factor calculation diagram.

CRI shows the ability of a light source's accurate colour rendering ability in comparison to a daylight reference source which has same correlated color temperature [77]. CCT refers to a light source's "warmth" or "coolness" and is measured in kelvin (K). Light is reddish when CCT is low, bluish white for high CCT and middle range of CCT presents neutral colour. CCT within the range between 3000 K-7500 K is preferred for transmitted daylight. However, it was found that 17000 K light improved subjective alertness and performance more strongly than 4000 K or 2900 K [78,79]. CRI [80] and CCT [81] are given by equations 8 and 9 respectively. Table 5 indicates the different CRI level.

$$CRI = \frac{1}{8}\sum_{i=1}^{8}\left[100 - 4.6\ \left\{\sqrt{(U^*_{t,i} - U^*_{r,i})^2 + (V^*_{t,i} - V^*_{r,i})^2 + (W^*_{t,i} - W^*_{r,i})^2}\right\}\right] \tag{8}$$

$$CCT = 449n^3 + 3525n^2 + 6823.3n + 5520.33 \tag{9}$$

Conversion into the CIE 1964 uniform colour space system for each test colours the conversion is performed using colour space system $W^*_{t,i}$ , $U^*_{t,i}$ , $V^*_{t,i}$ whereas $W^*_{r,i}$ , $U^*_{r,i}$ , $V^*_{r,i}$ represents for each test colours, lighted by the standard illuminant D65 without the glazing. where $n = \frac{(x - 0.3320)}{(0.1858 - y)}$ and x, y chromacity coordinate. Details of these parameters can be found elsewhere [82].

Table 5: Different quality of levels for a range of CRI.

| Rang of CRI ($R_a$) | Quality |
|---|---|
| ≥ 95 | Best |
| 95 > Ra > 90 | Good |
| where 90 > Ra > 80 | Reasonable |
| Ra ≤ 80 | Unreasonable |

## 3. Results and discussions

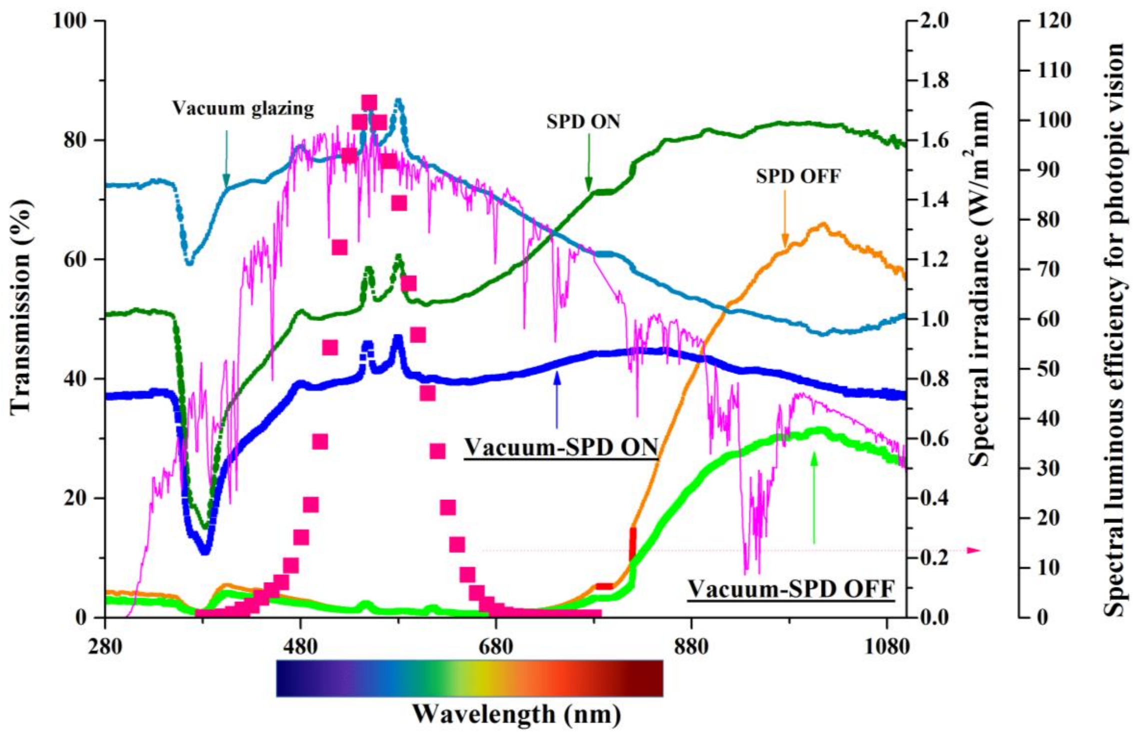

Figure 6: Transmission of SPD-vacuum glazing's switched ON transparent state and switched OFF opaque state.

Figure 6 shows the spectral transmission of SPD-vacuum glazing in its opaque and transparent states. For comparison, the transmission of SPD glazing, and vacuum glazing are also included. In the visible region, vacuum glazing has higher visible transmission which is 73%. Due to the presence of low-e coating, transmission in the NIR region is lower than visible region for vacuum glazing. SPD glazing has low control over NIR part compared to vacuum glazing. Thus, the addition of SPD-vacuum glazing shows lower NIR transmission compared to single SPD glazing but higher NIR compared to vacuum glazing. Different UV, the visible and solar transmission of all glazings are listed in Table 6.

Table 6: Transmission range of different glazing

| Glazing types | Visible transmission (%) | UV transmission (%) | Solar transmission (%) |
|---|---|---|---|
| SPD-vacuum ON | 38 | 32.4 | 39 |
| SPD-vacuum OFF | 2 | 2.28 | 11 |
| SPD ON | 53 | 44.24 | 63 |
| SPD OFF | 3 | 3.36 | 21 |
| Vacuum | 73 | 69.9 | 65 |

Solar factors and protection factors of SPD-vacuum glazing were calculated using equations 1, 3 and 4 and are summarised in Table 7. SPD-vacuum glazing SF varied from 0.38 at opaque state to 0.51 at transparent state. Intermediate controllable switching property of SPD [24] glazing enables SPD-vacuum glazing a potential alternative to control the SF of a building which can trim down the building energy. The presence of low-e coating in vacuum glazing allows low NIR transmission which provided low SF. SSPF and SMRF both were high and near to 1 for SPD-vacuum OFF state which indicates that the opaque state had higher UV control. SPD glazing switched ON and OFF states and SPD-vacuum glazing switched ON and OFF state showed different *U*-values. Variation for SPD glazing was due to control of entering solar energy in two different states. Lower *U*-value was found for SPD-vacuum combined system because vacuum glazing possesses higher heat insulation property.

Table 7: Protection factor for different glazing, overall heat transfer coefficient, and solar factor for SPD-vacuum opaque and transparent state and SPD glazing and Vacuum glazing.

| Glazing types | SSPF | $F_{sd}$ | SMRF | $\tau_{da}$ | SF | *U*-value (W/m$^2$K) |
|---|---|---|---|---|---|---|
| SPD-Vacuum ON | 61.2 | 38.8 | 54.39 | 45.61 | 0.51 | 1.16 [51] |
| SPD-Vacuum OFF | 96.72 | 3.28 | 97.15 | 2.85 | 0.38 | 1.0 [51] |
| SPD ON | 97.73 | 2.27 | 97.88 | 2.12 | 0.71 | 5.9 [25] |
| SPD OFF | 71.53 | 28.47 | 65.47 | 34.53 | 0.70 | 5.02 [26] |
| Vacuum | 30.95 | 69.05 | 25.61 | 74.39 | 0.30 | 1.4 [36] |

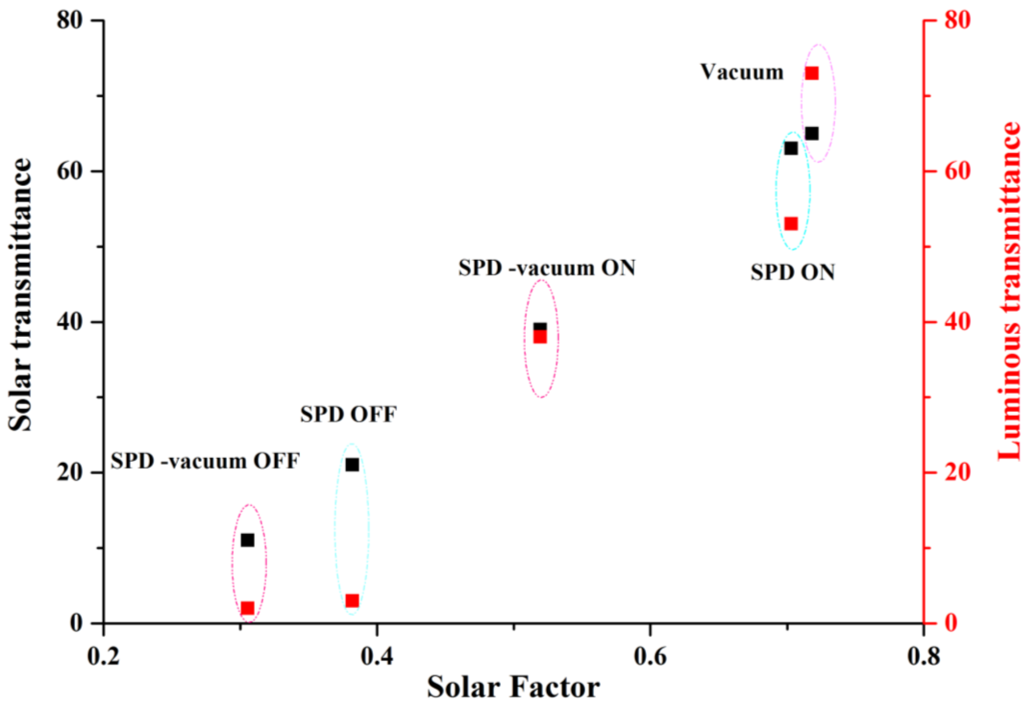


Figure 7: Solar factor, solar transmittance, and luminous transmittance of SPD -vacuum and SPD glazing for its opaque and transparent states and vacuum glazing.

Figure 7 illustrates the relation between solar factor and solar and luminous transmittance for SPD-vacuum opaque and transparent states. For comparison SPD glazing and vacuum glazing's results are also included. Contrast ratio (ratio of minimum and maximum transmittance) for solar transmission of SPD-vacuum glazing was 1:3.5 and for luminous transmission was 1:19. It is evident from the contrast ratio that visible transmission changed in higher order while the change of solar transmission was low between two states. Lower changes occurred for solar transmission as SPD opaque state blocks mostly the visible transmission. Thus, the difference between the solar and luminous transmission of SPD-vacuum transparent state in Figure 7 was also low.

Figure 8 shows the indoor test cell temperature for combined SPD-vacuum glazing for its opaque and transparent state and for comparison, SPD glazing, and vacuum glazing's test cell temperature are also added. Test cell temperature changed with the diurnal ambient condition (solar radiation and ambient temperature). Test cell temperature for vacuum glazing was lower than SPD glazing' opaque and transparent in both states. This was due to the presence of low-e coating in vacuum glazing which restricts to enter the NIR part of solar radiation inside the test cell. As expected, combined SPD-vacuum glazing provided lower temperature for both opaque and transparent conditions.

Figure 9 shows the thermal comfort level of SPD-vacuum glazing. This comfort was evaluated using indoor room temperature, incident solar radiation and ambient temperature from Figure 8 and using equation 5. Both opaque and transparent states showed allowable thermal comfort from early morning to afternoon time while mean ambient was $18^0$C. However neutral feeling was achieved for a short period of time.

Present thermal comfort equation was developed based on a conducted study with subjects aged between 20-25 years old, while the number of 60 years old people in the world is now doubled compared to 1980. Also, involved clothing insulation, metabolic rate, and environmental parameters are influenced by cultural, climatic, social and contextual dimensions [83]. The investigated PMV-PPD was developed by conducting experiments on North American and European people in climate chambers. Theoretical study and real-time study will be different as an less energy-hungry or energy-efficient building does not always lead to good occupancy satisfaction [84]. Thus, standard parameters may affect the real-time results [85] and variation may occur between experimental and simulation work.

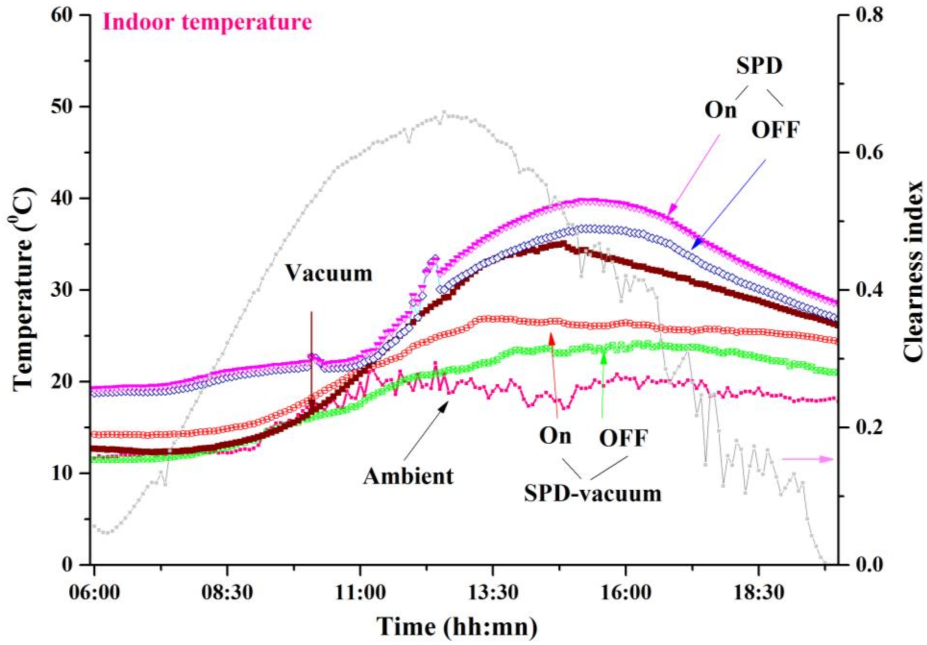


Figure 8: Indoor test cell temperature for vacuum glazing, SPD glazing and SPD-vacuum glazing opaque and transparent state while test cell and glazing ratio were 1:9 for clear sunny day at temperate climate.

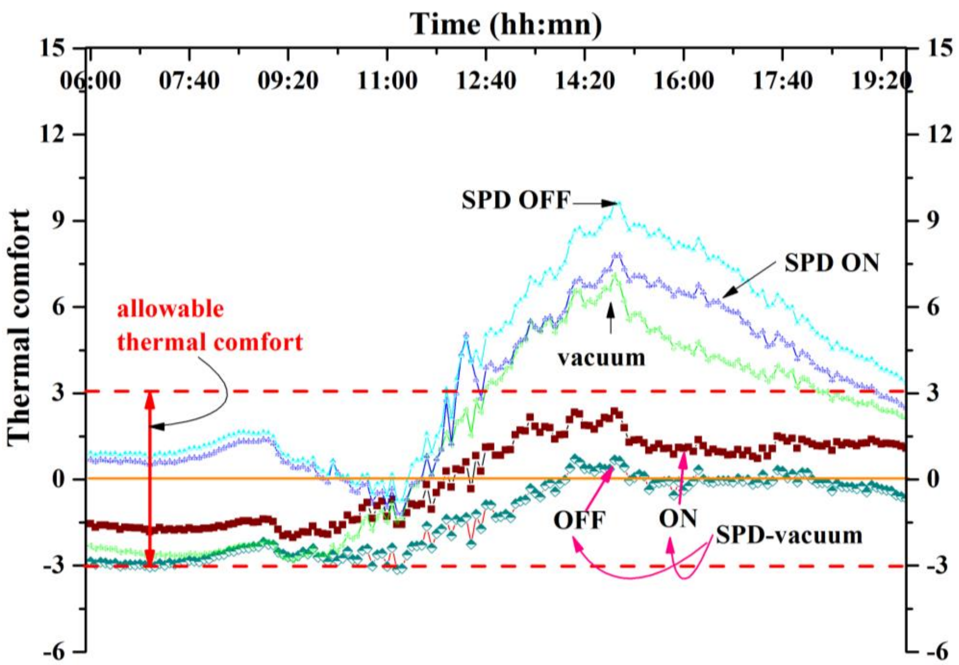


Figure 9: Diurnal variation of thermal comfort for SPD -vacuum opaque (OFF) and transparent (ON) states.

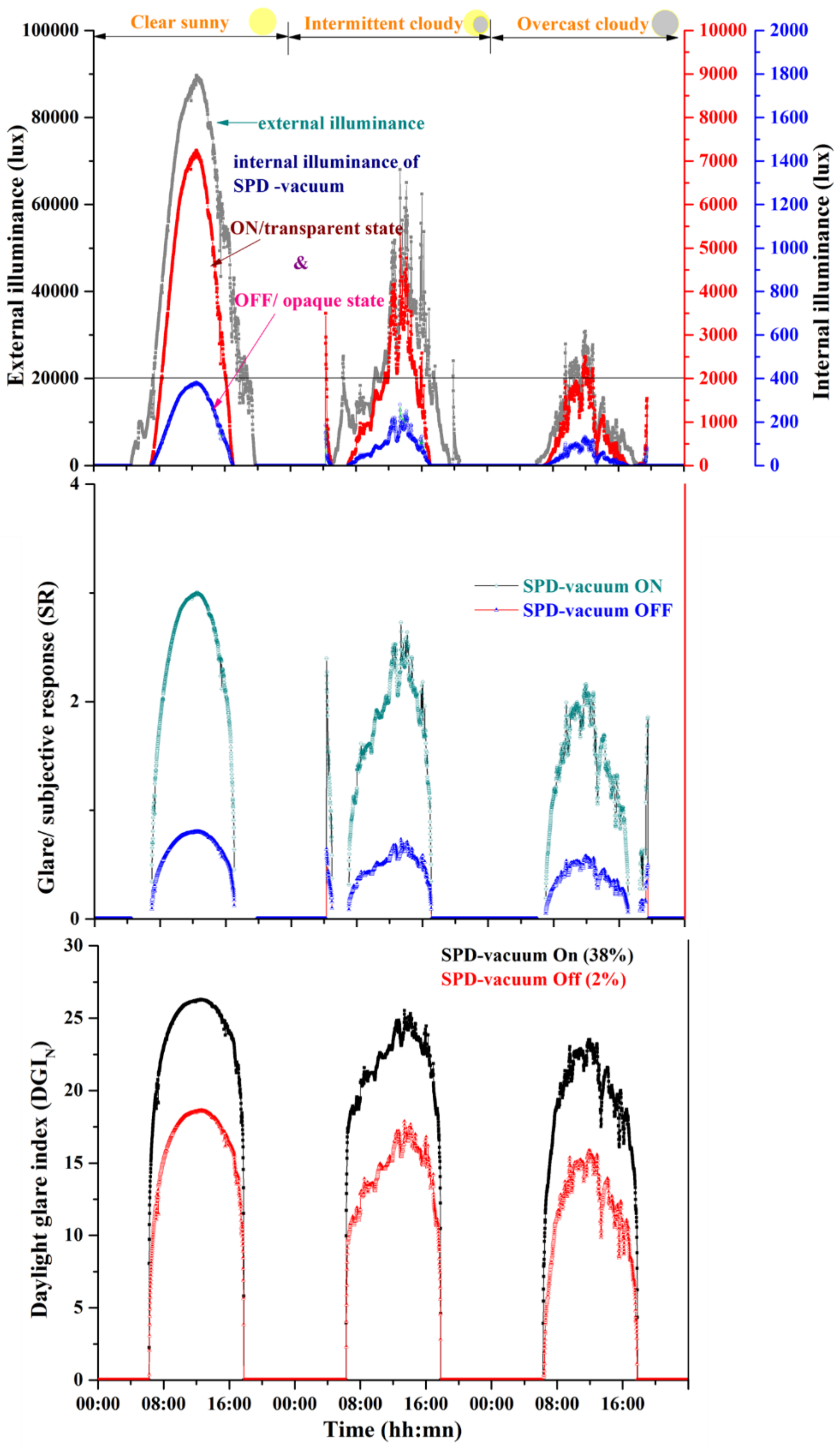


Figure 10: External illuminance, internal illuminance and subjective rating and daylight glare index for SPD-vacuum opaque and transparent state for three different sky conditions at temperate climate.

Figure 10 shows the external illuminance, internal illuminance and SR and daylight glare control potential for SPD-vacuum glazing's opaque and transparent state at the temperate climate for three different typical clear sunny, intermediate cloudy and overcast cloudy day. Vacuum glazing offers similar transmittance to double glazing thus is not included in this section [36] and SPD glazing's daylight performance can be found [27].

Internal illuminance ratio between the transparent and opaque state of SPD-vacuum glazing for three different states was 1.19 at 12:00 pm. The equal ratio was found between opaque and transparent state of luminous transmission for SPD–vacuum glazing. SPD –vacuum OFF state always provided 2000 lux internal illuminance which meets the UDI criteria for a clear sunny day. However, this glazing was not able to allow sufficient light for an overcast day and OFF state. Diurnal SR was calculated using equation 7 which showed that, for a clear sunny day, SPD-vacuum opaque state provided acceptable range before 10 am. At the mid-day period, SR range for the clear sunny day was higher however, for intermittent and cloudy day SR range was under acceptable range. It can also be added that intermediate transmission property of SPD-vacuum glazing enables its operation, for a clear sunny day to meet UDI level and SR by reducing the applied voltage level.

Daylight glare index for a clear sunny day using SPD –vacuum transparent state glazing was always below 26 which is the threshold limit of intolerable glare while the opaque state was above 17 at 12 pm. Thus, at higher exterior illuminance level during mid-day, SPD –vacuum glazing's opaque and transparent both states allowed comfortable daylight and offer visual comfort to occupant. Therefore, it can be concluded that for this temperate climatic condition, switch ON, OFF and intermediate states can offer potential visual comfort, however a choice of states depend on local climate and occupant choices.

CRI of SPD-vacuum transparent and opaque states was 94.83 and 66.72, while CCT was 5786.18 K and 45349.02 K respectively. Such glazing in fact can change the colour temperature in a wide range (e.g. from 45349.02 K to 5786.18 K) which thus results in a thermal feeling from colder to neutral, switching from opaque to transparent state. Transmission of SPD-vacuum glazing varies with incident angle [52]. Thus, angular transmittance has an influence on glazing performance and specifically for the vertical glazing. CCT and CRI for SPD –vacuum glazing was measured while incident solar radiation creates a zero-tilt angle. At $13^0$ incident angle, SPD-vacuum transparent state's transmission was 37% and opaque state had 1.8% transmission [52]. Therefore, it may be considered that CCT and CRI will vary with the variation of transmission. However it has to be kept into mind that CCT and CRI do not depend on single transmittance values but a spectral dependent values which need illuminant D65(λ) spectral power distribution and the photopic luminous efficiency function V(λ) for evaluation [86]. From CCT, CRI and glare analysis, SPD –vacuum transparent state is preferable for visual comfort as CRI and CCT are not attainable in the opaque state. However, for large scale integration, continuous power is required to achieve a transparent state for this glazing which in turn may enhance the building's energy demand.

## 4. Conclusions

In this work, SPD-vacuum glazing was employed to understand the potential of visual comfort and thermal comfort for a temperate climate. SPD glazing is smart switchable electrically activated which has switched ON transparent and switched OFF opaque states and has the ability to modulate the visible light. On the other hand, vacuum glazing offers control over near-infrared and controls heat losses from interior to exterior. A combination of them creates switchable, low heat loss adaptive SPD-vacuum glazing for low energy building integration. In this work, combined SPD-vacuum glazing changed its states from 2% to 38% when 110 V AC power supply was applied. Solar heat gain of this glazing which varied between 0.31 to 0.58 was calculated from the indoor spectral transmission. Thermal comfort was evaluated by using PMV-PPD methods and found to be suitable for both states of this glazing while external ambient was a clear sunny day and mean ambient was $18^0$C. Visual comfort was predicted using useful daylight illuminance, glare and colour properties analysis. For a clear sunny day, opaque states of this glazing provided 2000 lux at 12 am. However opaque state did not allow suitable daylight on a typical overcast day. Colour properties analysis showed that CRI of 94.83 and CCT of 5786.18 K both are suitable when a continuous power supply is given for a transparent state.

## CRediT author statement

**Srijita Nundy:** Software, Validation, Data curation, Writing- Original draft preparation, **Aritra Ghosh:** Conceptualization, Methodology, Writing- Reviewing and Editing, Project administration, Supervision


## Acknowledgement

This work did not receive any funding. The authors declare that they have no known competing financial interests or personal relationships that could have appeared to influence the work reported in this paper.


## Reference


[1] F. Zhang, R. de Dear, P. Hancock, Effects of moderate thermal environments on cognitive performance: A multidisciplinary review, Appl. Energy. 236 (2019) 760–777. doi:10.1016/j.apenergy.2018.12.005.

[2] A.K. Mishra, M.G.L.C. Loomans, J.L.M. Hensen, Thermal comfort of heterogeneous and dynamic indoor conditions — An overview, Build. Environ. 109 (2016) 82–100. doi:10.1016/j.buildenv.2016.09.016.

[3] P. Xue, C.M. Mak, Y. Huang, Quantification of luminous comfort with dynamic daylight metrics in residential buildings, Energy Build. 117 (2016) 99–108. doi:10.1016/j.enbuild.2016.02.026.

[4] L.A. López-Pérez, J.J. Flores-Prieto, C. Ríos-Rojas, Adaptive thermal comfort model for educational buildings in a hot-humid climate, Build. Environ. 150 (2019) 181–194. doi:10.1016/j.buildenv.2018.12.011.

[5] Z. Wang, R. De Dear, M. Luo, B. Lin, Y. He, A. Ghahramani, Individual di ff erence in thermal comfort : A literature review, 138 (2018) 181–193. doi:10.1016/j.buildenv.2018.04.040.

[6] S.D. Rezaei, S. Shannigrahi, S. Ramakrishna, A review of conventional, advanced, and smart glazing technologies and materials for improving indoor environment, Sol. Energy Mater. Sol. Cells. 159 (2017) 26–51. doi:10.1016/j.solmat.2016.08.026.

[7] G. Gorgolis, D. Karamanis, Solar energy materials for glazing technologies, Sol. Energy Mater. Sol. Cells. 144 (2016) 559–578. doi:10.1016/j.solmat.2015.09.040.

[8] W.J. Hee, M.A. Alghoul, B. Bakhtyar, O. Elayeb, M.A. Shameri, M.S. Alrubaih, K. Sopian, The role of window glazing on daylighting and energy saving in buildings, Renew. Sustain. Energy Rev. 42 (2015) 323–343. doi:10.1016/j.rser.2014.09.020.

[9] E.J. Gago, T. Muneer, M. Knez, H. Köster, Natural light controls and guides in buildings. Energy saving for electrical lighting, reduction of cooling load, Renew. Sustain. Energy Rev. 41 (2015) 1–13. doi:10.1016/j.rser.2014.08.002.

[10] A. Ghosh, B. Norton, Advances in switchable and highly insulating autonomous (self-powered) glazing systems for adaptive low energy buildings, Renew. Energy. 126 (2018)

1003–1031. doi:10.1016/j.renene.2018.04.038.

[11] R. Liang, Y. Sun, M. Aburas, R. Wilson, Y. Wu, Evaluation of the thermal and optical performance of thermochromic windows for office buildings in China, Energy Build. 176 (2018) 216–231. doi:10.1016/j.enbuild.2018.07.009.

[12] D. Zhao, G. Zhang, X. Zhang, D. Li, Optical properties of paraffin at temperature range from 40 to 80 °C, Optik (Stuttg). 157 (2018) 184–189. doi:10.1016/j.ijleo.2017.11.093.

[13] M. Hočevar, U. Opara Krašovec, A photochromic single glass pane, Sol. Energy Mater. Sol. Cells. 186 (2018) 111–114. doi:10.1016/j.solmat.2018.06.035.

[14] H. Kim, D. Ge, E. Lee, S. Yang, Multistate and On-Demand Smart Windows, 1803847 (2018). doi:10.1002/adma.201803847.

[15] A. Ghosh, B. Norton, Optimization of PV powered SPD switchable glazing to minimise probability of loss of power supply, Renew. Energy. 131 (2019) 993–1001. doi:10.1016/j.renene.2018.07.115.

[16] A. Ghosh, B. Norton, Interior colour rendering of daylight transmitted through a suspended particle device switchable glazing, Sol. Energy Mater. Sol. Cells. 163 (2017) 218–223. doi:10.1016/j.solmat.2017.01.041.

[17] H. Hakemi, Polymer-dispersed liquid crystal technology 'industrial evolution and current market situation,' Liq. Cryst. Today. 26 (2017) 70–73. doi:10.1080/1358314X.2017.1359143.

[18] C.P. Films, M. Oh, C. Lee, J. Park, K. Lee, S. Tae, Evaluation of Energy and Daylight Performance of Old O ffi ce Buildings in South Korea with Curtain Walls Remodeled Using Polymer Dispersed Liquid, (2019).

[19] A. Ghosh, B. Norton, T.K. Mallick, Influence of atmospheric clearness on PDLC switchable glazing transmission, Energy Build. 172 (2018) 257–264. doi:10.1016/j.enbuild.2018.05.008.

[20] A. Ghosh, T.K. Mallick, Evaluation of optical properties and protection factors of a PDLC switchable glazing for low energy building integration, Sol. Energy Mater. Sol. Cells. (2017) 0–1. doi:10.1016/j.solmat.2017.10.026.

[21] B.-S. Yu, E.-S. Kim, Y.-W. Lee, <title>Developments in suspended particle devices (SPD)</title>, Opt. Mater. Technol. Energy Effic. Sol. Energy Convers. XV. 3138 (2005) 217–225. doi:10.1117/12.279204.

[22] D. Barrios, R. Vergaz, J.M. Sanchez-Pena, C.G. Granqvist, G.A. Niklasson, Toward a quantitative model for suspended particle devices: Optical scattering and absorption coefficients, Sol. Energy Mater. Sol. Cells. 111 (2013) 115–122. doi:10.1016/j.solmat.2012.12.012.

[23] D. Barrios, R. Vergaz, J.M. Sánchez-Pena, B. García-Cámara, C.G. Granqvist, G.A. Niklasson, Simulation of the thickness dependence of the optical properties of suspended particle devices, Sol. Energy Mater. Sol. Cells. 143 (2015) 613–622. doi:10.1016/j.solmat.2015.05.044.

[24] A. Ghosh, B. Norton, Durability of switching behaviour after outdoor exposure for a suspended particle device switchable glazing, Sol. Energy Mater. Sol. Cells. 163 (2017) 178–184. doi:10.1016/j.solmat.2017.01.036.

[25] A. Ghosh, B. Norton, A. Duffy, Measured overall heat transfer coefficient of a suspended particle device switchable glazing, Appl. Energy. 159 (2015) 362–369. doi:10.1016/j.apenergy.2015.09.019.

[26] A. Ghosh, B. Norton, A. Duffy, Behaviour of a SPD switchable glazing in an outdoor test cell with heat removal under varying weather conditions, Appl. Energy. 180 (2016) 695–706. doi:10.1016/j.apenergy.2016.08.029.

[27] A. Ghosh, B. Norton, A. Duffy, Daylighting performance and glare calculation of a suspended particle device switchable glazing, Sol. Energy. 132 (2016) 114–128. doi:10.1016/j.solener.2016.02.051.

[28] A. Ghosh, B. Norton, A. Duffy, Effect of sky conditions on light transmission through a suspended particle device switchable glazing, Sol. Energy Mater. Sol. Cells. 160 (2017) 134–140. doi:10.1016/j.solmat.2016.09.049.

[29] A. Ghosh, B. Norton, A. Duffy, First outdoor characterisation of a PV powered suspended particle device switchable glazing, Sol. Energy Mater. Sol. Cells. 157 (2016) 1–9. doi:10.1016/j.solmat.2016.05.013.

[30] H. Khandelwal, R.C.G.M. Loonen, J.L.M. Hensen, M.G. Debije, A.P.H.J. Schenning, Electrically switchable polymer stabilised broadband infrared reflectors and their potential as smart windows for energy saving in buildings, Sci. Rep. 5 (2015) 2–10. doi:10.1038/srep11773.

[31] H. Khandelwal, E.P.A. van Heeswijk, A.P.H.J. Schenning, M.G. Debije, Paintable temperature-responsive cholesteric liquid crystal reflectors encapsulated on a single flexible polymer substrate, J. Mater. Chem. C. 328 (2019). doi:10.1039/C9TC02011J.

[32] B. Cerne, A. Kralj, M. Drev, M. Žnidarši, J. Hafner, B. Petter, Energy & Buildings Investigations of 6-pane glazing : Properties and possibilities, 190 (2019) 61–68. doi:10.1016/j.enbuild.2019.02.033.

[33] M. Zinzi, G. Rossi, A.M. Anderson, M.K. Carroll, E. Moretti, Optical and visual experimental characterization of a glazing system with monolithic silica aerogel, Sol. Energy. 183 (2019) 30–39. doi:10.1016/j.solener.2019.03.013.

[34] X. Zhou, Y. Huang, H. Wu, Y. Lv, Y. Liu, R. Huang, T. Xu, Quantitative research on the influence of particle size and filling thickness on aerogel glazing performance, Energy Build. 174 (2018) 190–198. doi:10.1016/j.enbuild.2018.06.026.

[35] S. Memon, Y. Fang, P.C. Eames, The influence of low-temperature surface induction on evacuation, pump-out hole sealing and thermal performance of composite edge-sealed vacuum insulated glazing, Renew. Energy. 135 (2019) 450–464. doi:10.1016/j.renene.2018.12.025.

[36] A. Ghosh, B. Norton, A. Duffy, Measured thermal & daylight performance of an evacuated glazing using an outdoor test cell, Appl. Energy. 177 (2016) 196–203. doi:10.1016/j.apenergy.2016.05.118.

[37] B. Büttner, J. Nauschütz, U. Heinemann, G. Reichenauer, C. Scherdel, H. Weinläder, S. Weismann, D. Buck, A. Beck, Evacuated Glazing with Silica Aerogel Spacers, (2019) 1–8. doi:10.18086/eurosun2018.06.17.

[38] E. Cuce, P.M. Cuce, Vacuum glazing for highly insulating windows: Recent developments and future prospects, Renew. Sustain. Energy Rev. 54 (2016) 1345–1347. doi:10.1016/j.rser.2015.10.134.

[39] P.C. Eames, Vacuum glazing: Current performance and future prospects, Vacuum. 82 (2008) 717–722. doi:10.1016/j.vacuum.2007.10.017.

[40] Y. Fang, T. Hyde, P.C. Eames, N. Hewitt, Theoretical and experimental analysis of the vacuum

pressure in a vacuum glazing after extreme thermal cycling, Sol. Energy. 83 (2009) 1723–1730. doi:10.1016/j.solener.2009.03.017.

[41] Y. Fang, T.J. Hyde, F. Arya, N. Hewitt, P.C. Eames, B. Norton, S. Miller, Indium alloy-sealed vacuum glazing development and context, Renew. Sustain. Energy Rev. 37 (2014) 480–501. doi:10.1016/j.rser.2014.05.029.

[42] S. Memon, Experimental measurement of hermetic edge seal's thermal conductivity for the thermal transmittance prediction of triple vacuum glazing, Case Stud. Therm. Eng. 10 (2017) 169–178. doi:10.1016/j.csite.2017.06.002.

[43] Y. Fang, P.C. Eames, B. Norton, T.J. Hyde, J. Zhao, J. Wang, Y. Huang, Low emittance coatings and the thermal performance of vacuum glazing, Sol. Energy. 81 (2007) 8–12. doi:10.1016/j.solener.2006.06.011.

[44] P.W. Griffiths, M. Di Leo, P. Cartwright, P.C. Eames, P. Yianoulis, G. Leftheriotis, B. Norton, Fabrication of evacuated glazing at low temperature, Sol. Energy. 63 (1998) 243–249. doi:10.1016/S0038-092X(98)00019-X.

[45] R.E. Collins, S.J. Robinson, Evacuated glazing, Sol. Energy. 47 (1991) 27–38. doi:10.1016/0038-092X(91)90060-A.

[46] R.E. Collins, G.M. Turner, A.C. Fischer-Cripps, J.Z. Tang, T.M. Simko, C.J. Dey, D.A. Clugston, Q.C. Zhang, J.D. Garrison, Vacuum glazing-A new component for insulating windows, Build. Environ. 30 (1995) 459–492. doi:10.1016/0360-1323(95)00025-2.

[47] Y. Fang, P.C. Eames, B. Norton, T.J. Hyde, Experimental validation of a numerical model for heat transfer in vacuum glazing, Sol. Energy. 80 (2006) 564–577. doi:10.1016/j.solener.2005.04.002.

[48] Y. Fang, T. Hyde, N. Hewitt, P.C. Eames, B. Norton, Comparison of vacuum glazing thermal performance predicted using two- and three-dimensional models and their experimental validation, Sol. Energy Mater. Sol. Cells. 93 (2009) 1492–1498. doi:10.1016/j.solmat.2009.03.025.

[49] A. Ghosh, B. Norton, A. Duffy, Effect of sky clearness index on transmission of evacuated (vacuum) glazing, Renew. Energy. 105 (2017) 160–166. doi:10.1016/j.renene.2016.12.056.

[50] A. Ghosh, S. Sundaram, T.K. Mallick, Colour properties and glazing factors evaluation of multicrystalline based semi-transparent Photovoltaic-vacuum glazing for BIPV application, Renew. Energy. 131 (2019) 730–736. doi:10.1016/j.renene.2018.07.088.

[51] A. Ghosh, B. Norton, A. Duffy, Measured thermal performance of a combined suspended particle switchable device evacuated glazing, Appl. Energy. 169 (2016) 469–480. doi:10.1016/j.apenergy.2016.02.031.

[52] A. Ghosh, B. Norton, A. Duffy, Effect of atmospheric transmittance on performance of adaptive SPD-vacuum switchable glazing, Sol. Energy Mater. Sol. Cells. 161 (2017) 424–431. doi:10.1016/j.solmat.2016.12.022.

[53] P.O. Fanger, J. Toftum, Extension of the PMV model to non-air-conditioned buildings in warm climates, 34 (2002) 533–536.

[54] M.C. Singh, S.N. Garg, R. Jha, Different glazing systems and their impact on human thermal comfort-Indian scenario, Build. Environ. 43 (2008) 1596–1602. doi:10.1016/j.buildenv.2007.10.004.

[55] S. Chaiyapinunt, B. Phueakphongsuriya, K. Mongkornsaksit, N. Khomporn, Performance rating

of glass windows and glass windows with films in aspect of thermal comfort and heat transmission, Energy Build. 37 (2005) 725–738. doi:10.1016/j.enbuild.2004.10.008.

[56] W. He, Y.X. Zhang, W. Sun, J.X. Hou, Q.Y. Jiang, J. Ji, Experimental and numerical investigation on the performance of amorphous silicon photovoltaics window in East China, Build. Environ. 46 (2011) 363–369. doi:10.1016/j.buildenv.2010.07.030.

[57] D. Biswas, C. Szocs, R. Chacko, B. Wansink, Shining Light on Atmospherics: How Ambient Light Influences Food Choices, J. Mark. Res. 54 (2016) 111–123. doi:10.1509/jmr.14.0115.

[58] K.C.H.J. Smolders, Y.A.W. de Kort, Bright light and mental fatigue: Effects on alertness, vitality, performance and physiological arousal, J. Environ. Psychol. 39 (2014) 77–91. doi:10.1016/j.jenvp.2013.12.010.

[59] A. Piccolo, F. Simone, Effect of switchable glazing on discomfort glare from windows, Build. Environ. 44 (2009) 1171–1180. doi:10.1016/j.buildenv.2008.08.013.

[60] A. Ghosh, B. Norton, T.K. Mallick, Daylight characteristics of a polymer dispersed liquid crystal switchable glazing, Sol. Energy Mater. Sol. Cells. 174 (2018) 572–576. doi:10.1016/j.solmat.2017.09.047.

[61] M.C. Peel, B.L. Finlayson, T.A. McMahon, Updated world map of the Köppen-Geiger climate classification, Hydrol. Earth Syst. Sci. 11 (2007) 1633–1644. doi:10.5194/hess-11-1633-2007.

[62] M. Kottek, J. Grieser, C. Beck, B. Rudolf, F. Rubel, World Map of the Koppen-Geiger climate classification update, Meteorol. Zeitschrift. 15 (2006) 259–263. doi:10.1127/0941-2948/2006/0130.

[63] A. Albatayneh, D. Alterman, A. Page, B. Moghtaderi, Energy for Sustainable Development Development of a new metric to characterise the buildings thermal performance in a temperate climate, Energy Sustain. Dev. 51 (2019) 1–12. doi:10.1016/j.esd.2019.04.002.

[64] L. Gill, J. Mac Mahon, K. Ryan, The performance of an evacuated tube solar hot water system in a domestic house throughout a year in a northern maritime climate (Dublin), Sol. Energy. 137 (2016) 261–272. doi:10.1016/j.solener.2016.07.052.

[65] Y. Wang, Y. Liu, C. Song, J. Liu, Appropriate indoor operative temperature and bedding micro climate temperature that satisfies the requirements of sleep thermal comfort, Build. Environ. 92 (2015) 20–29. doi:10.1016/j.buildenv.2015.04.015.

[66] B.P. Jelle, Solar radiation glazing factors for window panes, glass structures and electrochromic windows in buildings - Measurement and calculation, Sol. Energy Mater. Sol. Cells. 116 (2013) 291–323. doi:10.1016/j.solmat.2013.04.032.

[67] A. Qahtan, S.P. Rao, N. Keumala, The effectiveness of the sustainable flowing water film in improving the solar-optical properties of glazing in the tropics, Energy Build. 77 (2014) 247–255. doi:10.1016/j.enbuild.2014.03.051.

[68] ASHRAE-55, Ashrae_Standard_55_2013_Thermal.Pdf, (2010) 5.

[69] ISO, International Standard Iso, 2009 (2009).

[70] A. Nabil, J. Mardaljevic, Useful daylight illuminances: A replacement for daylight factors, Energy Build. 38 (2006) 905–913. doi:10.1016/j.enbuild.2006.03.013.

[71] E.S. Lee, D.L. DiBartolomeo, Application issues for large-area electrochromic windows in commercial buildings, Sol. Energy Mater. Sol. Cells. 71 (2002) 465–491. doi:10.1016/S0927-0248(01)00101-5.

[72] E.S. Lee, D.L. DiBartolomeo, S.E. Selkowitz, The effect of venetian blinds on daylight photoelectric control performance, J. Illum. Eng. Soc. 28 (1999) 3–23. doi:10.1080/00994480.1999.10748247.

[73] A.A. Nazzal, A New Daylight Glare Evaluation Method., J. Light Vis. Environ. 24 (2000) 19–27. doi:10.2150/jlve.24.2_19.

[74] A.A. Nazzal, A new evaluation method for daylight discomfort glare, Int. J. Ind. Ergon. 35 (2005) 295–306. doi:10.1016/j.ergon.2004.08.010.

[75] M. Sudan, G.N. Tiwari, Daylighting and energy performance of a building for composite climate: An experimental study, Alexandria Eng. J. 55 (2016) 3091–3100. doi:10.1016/j.aej.2016.08.014.

[76] A. Thanachareonkit, J.L. Scartezzini, M. Andersen, Comparing daylighting performance assessment of buildings in scale models and test modules, Sol. Energy. 79 (2005) 168–182. doi:10.1016/j.solener.2005.01.011.

[77] N. Aste, F. Leonforte, A. Piccolo, Color rendering performance of smart glazings for building applications, Sol. Energy. 176 (2018) 51–61. doi:10.1016/j.solener.2018.10.026.

[78] P.R. Mills, S.C. Tomkins, L.J.M. Schlangen, The effect of high correlated colour temperature office lighting on employee wellbeing and work performance., J. Circadian Rhythms. 5 (2007) 2. doi:10.1186/1740-3391-5-2.

[79] A.U. Viola, L.M. James, L.J.M. Schlangen, D.J. Dijk, Blue-enriched white light in the workplace improves self-reported alertness, performance and sleep quality, Scand. J. Work. Environ. Heal. 34 (2008) 297–306. doi:10.5271/sjweh.1268.

[80] C.I. De l'Eclairage, CIE 1988 2 spectral luminous efficiency function for photopic vision, 1990.

[81] C.S. McCamy, Correlated color temperature as an explicit function of chromaticity coordinates, Color Res. Appl. 17 (1992) 142–144. doi:10.1002/col.5080170211.

[82] A. Ghosh, P. Selvaraj, S. Sundaram, T.K. Mallick, The colour rendering index and correlated colour temperature of dye-sensitized solar cell for adaptive glazing application, Sol. Energy. 163 (2018) 537–544. doi:10.1016/j.solener.2018.02.021.

[83] R.J. de Dear, G.S. Brager, Developing an adaptive model of thermal comfort and preference, ASHRAE Trans. 104 (1998) 145–167.

[84] Å.L. Hauge, J. Thomsen, T. Berker, User evaluations of energy efficient buildings: Literature review and further research, Adv. Build. Energy Res. 5 (2011) 109–127. doi:10.1080/17512549.2011.582350.

[85] V. Soebarto, H. Zhang, S. Schiavon, A thermal comfort environmental chamber study of older and younger people, Build. Environ. 155 (2019) 1–14. doi:10.1016/J.BUILDENV.2019.03.032.

[86] M.K. Gunde, U.O. Krašovec, W.J. Platzer, Color rendering properties of interior lighting influenced by a switchable window, J. Opt. Soc. Am. A. 22 (2005) 416. doi:10.1364/JOSAA.22.000416.